The EMBO Journal (2004) 23, 1422–1432 | © 2004 European Molecular Biology Organization | All Rights Reserved 0261-4189/04
www.embojournal.org

THE EMBO JOURNAL

Structure of a kinesin microtubule depolymerization machine

Krista Shipley[1], Mohammad Hekmat-Nejad[2], Jennifer Turner[3,5], Carolyn Moores[4,6], Robert Anderson[2], Ronald Milligan[4], Roman Sakowicz[2] and Robert Fletterick[3,*]

[1]Graduate Group in Biophysics, University of California, San Francisco, CA, USA, [2]Cytokinetics Inc., South San Francisco, CA, USA, [3]Department of Biochemistry/Biophysics, University of California, San Francisco, CA, USA and [4]Department of Cell Biology, The Scripps Research Institute, La Jolla, CA, USA

With their ability to depolymerize microtubules (MTs), KinI kinesins are the rogue members of the kinesin family. Here we present the 1.6 Å crystal structure of a KinI motor core from *Plasmodium falciparum*, which is sufficient for depolymerization *in vitro*. Unlike all published kinesin structures to date, nucleotide is not present, and there are noticeable differences in loop regions L6 and L10 (the plus-end tip), L2 and L8 and in switch II (L11 and helix4); otherwise, the pKinI structure is very similar to previous kinesin structures. KinI-conserved amino acids were mutated to alanine, and studied for their effects on depolymerization and ATP hydrolysis. Notably, mutation of three residues in L2 appears to primarily affect depolymerization, rather than general MT binding or ATP hydrolysis. The results of this study confirm the suspected importance of loop 2 for KinI function, and provide evidence that KinI is specialized to hydrolyze ATP after initiating depolymerization.

The EMBO Journal (2004) **23**, 1422–1432. doi:10.1038/sj.emboj.7600165; Published online 18 March 2004
Subject Categories: structural biology; membranes & transport
Keywords: crystal; depolymerization; kinesin; microtubule; structure

Introduction

Each cell type in every eucaryotic organism contains multiple kinesin-superfamily members. To date, over 30 kinesins have been found in the human genome (Kinesin Homepage: http://www.proweb.org/kinesin/index.html). Although kinesin proteins differ widely in their cellular function, they all share the ability to modulate their interactions with microtubules (MTs) through binding and hydrolysis of ATP by their conserved catalytic core, which constitutes the major part of the kinesin motor domain (Vale and Fletterick, 1997). Some kinesins translocate cargo towards the plus ends of MTs; these kinesins have their motor domains at the N-terminus of their polypeptide chain, and are therefore classified into the KinN family (Vale *et al*, 1985; Vale and Fletterick, 1997). Other kinesins move in the opposite direction; these have their motor domain at the opposite C-terminus, and are called KinC motors (McDonald *et al*, 1990; Vale and Fletterick, 1997).

Kinesin subfamily KinI (termed so for the **I**nternal location of the motor domain) performs a completely different function: it initiates MT depolymerization instead of acting as a motor (Desai *et al*, 1999). MT depolymerization is involved in establishment and maintenance of the mitotic spindle and is vital for chromosome segregation during cell division (Inoué and Salmon, 1995; Rogers *et al*, 2004). The MT-depolymerizing activity is best understood for the KinI kinesins that localize to the kinetochore during mitosis; these are called XKCM1 in *Xenopus* (Desai *et al*, 1999; Kline-Smith and Walczak, 2002) and MCAK in mammals (Wordeman and Mitchison, 1995; Hunter *et al*, 2003). Kif2, another KinI kinesin type first found in murine brain (Aizawa *et al*, 1992), has also been shown to depolymerize MT *in vitro* (Desai *et al*, 1999). A recent study suggests that Kif2 plays a nonmitotic role in the development of the nervous system, by suppressing extension of superfluous branches at the cell edge of (post-mitotic) neurons (Homma *et al*, 2003).

KinI perturbs the MT polymerization and depolymerization cycle, which is controlled by the GTPase cycle of the individual α/β-tubulin heterodimers in the polymer (as reviewed in Desai and Mitchison, 1997). GTP-bound tubulin dimers are straight, and polymerize to form straight MTs, while free GDP-bound tubulin dimers are curved. Thus, a tubulin dimer in a MT would prefer to adopt a curved shape after hydrolyzing its GTP to GDP, but is kept straight by side-by-side (lateral) interactions with adjoining protofilaments. There are fewer of these stabilizing interactions at the ends of the MT, where at least one of the dimers has a single lateral interaction. Consequently, GTP hydrolysis in these exposed end tubulin dimers will lead to curvature and peeling away of their respective protofilaments, and the start of depolymerization.

In vivo, growth and decay of MTs are vital for many cellular processes, so there are many proteins known that regulate the onset of depolymerization (Walczak, 2000). Some, such as op18/stathmin, are thought to initiate depolymerization by activating GTP hydrolysis when they bind to the ends of MTs (Segerman *et al*, 2000). KinI likely employ a different mechanism, as they can depolymerize MTs stabilized by a nonhydrolyzable GTP analogue GMP-CPP (Desai *et al*, 1999; Moores *et al*, 2002; Hunter *et al*, 2003).

In trying to understand KinI, many important details of their function have been elucidated. In particular, KinI were

*Corresponding author. Department of Biochemistry & Biophysics, University of California, GH Rm. S412E, 600 16th Street, Suite #2240, San Francisco, CA, 94143-2240, USA. Tel.: +1 415 476 5080; Fax: +1 415 476 1902; E-mail: flett@msg.ucsf.edu
[5]Present address: Department of Biology, Box 731 Vassar College, 124 Raymond Avenue, Poughkeepsie, NY 12604-0731, USA
[6]Present address: School of Crystallography, Birkbeck College, University of London, Malet Street, London WC1E 7HX, UK

Received: 12 December 2003; accepted: 18 February 2004; published online: 18 March 2004

shown not to walk along the MT, but rather target directly to the MT ends (Desai *et al*, 1999) or reach the ends by rapid one-dimensional diffusion (Hunter *et al*, 2003). Like other kinesins, KinI are ATPases, but ATP hydrolysis is not necessary to disassemble MTs, because KinI bound to the nonhydrolyzable ATP analogue AMP-PNP can induce MT protofilament peeling (Desai *et al*, 1999; Moores *et al*, 2002). ATP hydrolysis appears necessary for KinI to release from free tubulin dimer, in order to rebind the MT and depolymerize in a catalytic fashion (Desai *et al*, 1999). This is analogous to conventional human kinesin (KHC), in which the power stroke, which propels the nonbound motor head forward, is induced by ATP binding, and ATP hydrolysis weakens the association with the MT (Rice *et al*, 1999). It also appears that hydrolysis occurs before release of the KinI–tubulin complex from the MT, because (full-length) MCAK has a higher ATPase activity in the presence of MTs than free tubulin (Hunter *et al*, 2003), and because AMPPNP-bound KinI forms rings from nonstabilized MTs (Moores *et al*, 2002).

Although KinI appear to function as dimers *in vivo*, KinI monomers were shown to be sufficient to depolymerize MT (Maney *et al*, 2001; Moores *et al*, 2002; Niederstrasser *et al*, 2002). XKCM1 dimers are also able to depolymerize antiparallel, zinc-stabilized tubulin macrotubes. The latter finding suggests that XKCM1 does not bind at the protofilament interface to tear it apart, but rather acts on a single protofilament (Niederstrasser *et al*, 2002). Limited proteolysis experiments showed that removal of the tubulin C-terminus reduced gliding kinesin processivity (Okada and Hirokawa, 2000; Thorn *et al*, 2000; Wang and Sheetz, 2000). Similar experiments showed that the C-terminal tubulin region, while dispensable for binding of KinI to MT, is necessary for MT depolymerization by KinI (Moores *et al*, 2002; Niederstrasser *et al*, 2002).

Plasmodium falciparum KinI can depolymerize MT *in vitro* as a monomer, using just the catalytic core domain with no N-terminal neck attached (Moores *et al*, 2002). However, the presence of the neck markedly increases the rate of depolymerization in the mammalian homologue MCAK (Maney *et al*, 2001). The role of the KinI neck is still under scrutiny, but it is generally thought that it might improve the efficiency of MT depolymerization by targeting the protein to MT ends. Alternatively, the presence of the neck could decrease the off rate from MTs, which would contribute to higher KinI activity found under physiological conditions (Ovechkina *et al*, 2002).

As the crystal structure of any kinesin motor in complex with tubulin is not yet available, our understanding of how kinesins interact with MTs is restricted to lower-resolution techniques, such as proteolytic mapping (Alonso *et al*, 1998), mutagenesis experiments (Woehlke *et al*, 1997) and fitting atomic coordinates of kinesin motor domains into electron density maps derived from EM experiments (Mandelkow and Hoenger, 1999; Kikkawa *et al*, 2001). As for KinI, the only prior information on how it specifically interacts with the MT has been obtained by inference from fitting crystallographic models of other kinesin motors into EM maps of KinI bound to MTs (Moores *et al*, 2002, 2003).

The most intriguing question to date about the Internal Kinesins is how the catalytic core alone, being almost identical in its primary structure to other kinesin core domains, can perform a function so different from the usual gliding motion. To understand better how KinI works, we determined the crystal structure of *P. falciparum* KinI catalytic core to 1.6 Å resolution. Furthermore, we mutated family-conserved residues to study how their loss affected protein activity. These combined studies identified structural elements of KinI that are important for MT depolymerization.

Results

Crystal structure of the KinI catalytic core

While several KinI have been characterized, for our structural studies we used the readily crystallizable catalytic core domain of the *P. falciparum* MCAK homologue (pKinI), which is sufficient to perform MT depolymerization *in vitro* (Moores *et al*, 2002). The pKinI catalytic core was expressed, purified and crystallized, and its structure was determined by molecular replacement, as described in Materials and methods. The current crystallographic model is refined to 1.6 Å with R/R_{free} values of 0.2023 and 0.2304 (Table I), and consists of 318 amino-acid residues (12 of the total 330 residues are disordered). The structure of pKinI (Figure 1) revealed a protein domain similar to the previously determined kinesin catalytic cores (Figure 2). Kinesin core structures are generally 'arrowhead' shaped, consisting of a central β-sheet region surrounded by α-helices, and have always been found complexed with adenosine nucleotide (Kull and Endow, 2002). The pKinI structure differs the most from previous kinesin models in that there is no nucleotide present in the ATP-binding site. Furthermore, in contrast to most kinesin structures, the switch II loop L11 of pKinI is ordered and forms a short two-turn helix. MT-binding loop L8 does not form a long strand pair pointing towards the MT-binding face, which is seen in most gliding kinesins. Instead, L8 appears to point in the opposite direction, although it is too disordered to resolve its structure completely.

Some features of the pKinI structure are not strictly unique, but are found in only a few kinesin structures. For example, the 'pointed tip' of the kinesin 'arrowhead' (loops L6 and

Table I Data collection and refinement statistics

Crystallization	
Space group	$P3_221$
Unit-cell dimensions	
a (Å)	105.59
c (Å)	84.77
Molecules per asymmetric unit	1
Resolution (Å)	1.6
Number of unique reflections	66077
Completeness (%)	91.5 (84.5)
R_{symm} (%)	4.8 (36.9)
$\langle I/\sigma(I)\rangle$	15.52 (1.75)
Refinement (24.9–1.60 Å)	
R	0.2023
R_{free}	0.2304
Rms deviation from ideality	
Bond length (Å)	0.022
Bond angle (deg)	1.871
Average *B* factor (Å^2)	27.0

Numbers in parentheses are for the last resolution shell (1.62–1.69 Å). $R_{symm} = \sum_h |I_h - I| / \sum_h I$, where (I) is the mean intensity of reflection h. R_{free} is for 5% of total reflections not included in the refinement.

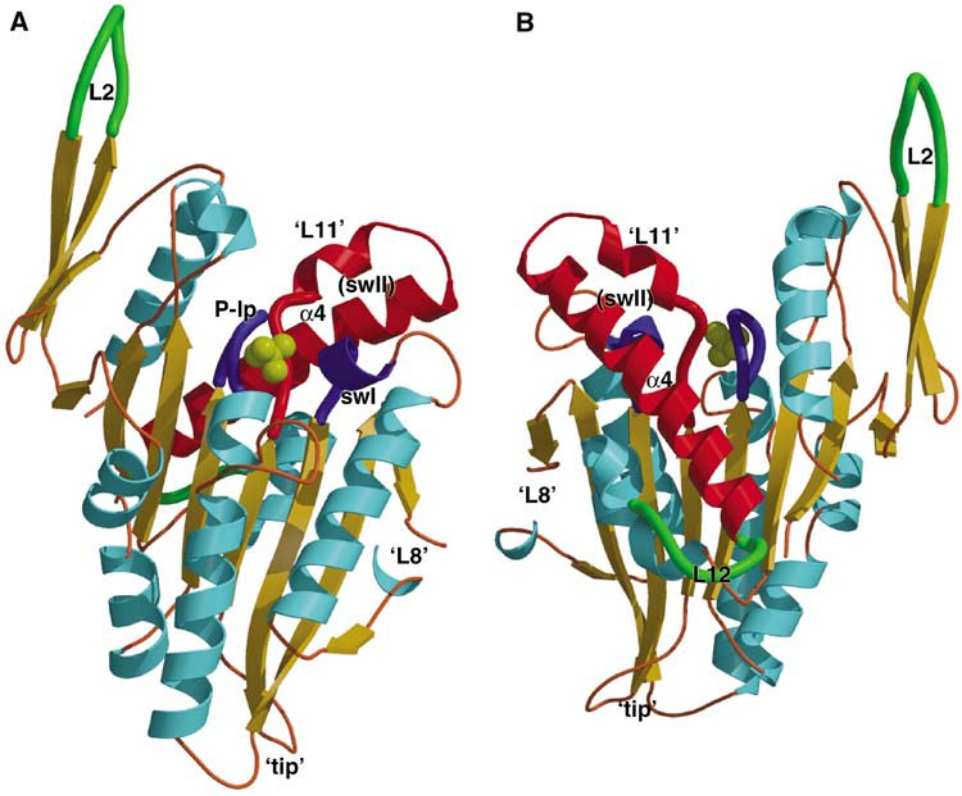

Figure 1 X-ray crystal structure (1.6 Å) of pKinI. Important areas for kinesin function are highlighted: part of the MT-binding surface (L2, L12) in green; blue nucleotide-binding pocket (P-loop, switch I); and red switch II (L11-α4), which contacts both the MT and the nucleotide. The sulfate found at the β-phosphate position is represented as yellow balls.

L10) is noticeably bent in the pKinI structure. In the recently solved Eg5 structure (Turner *et al*, 2001), this region is also bent, but in the opposite direction. MT-contacting L2 is noticeably longer in pKinI, although the same region in NCD and Eg5 approaches it in length. The long, MT-contacting switch II helix α4 is visible and structured for its entire length, a feature previously seen in the Kif1a-ADP structure (Kikkawa *et al*, 2001).

Nucleotide-binding pocket of pKinI

Prior to pKinI, all kinesins have been crystallized with an adenosine nucleotide bound, despite numerous attempts at crystallizing a nucleotide-free motor (Muller *et al*, 1999). Strikingly, the ATP-binding pocket of pKinI does not have a bound nucleotide (Figure 1). Although there is no continuous electron density consistent with the presence of the bound nucleotide, the nucleotide-binding site is not empty. Figure 3A shows the electron density (in green) found in the nucleotide-binding site of pKinI. For reference, ADP from the superposed Kif1A model is included (1I5S; Kikkawa *et al*, 2001). At the exact position of the β-phosphate found in other structures, crystalline pKinI contains a single sulfate ion, which is likely derived from the crystallization buffer (see Materials and methods). To confirm the absence of bound nucleotide, we performed one round of refinement after replacing the sulfate ion with ADP. As illustrated in Figure 3B, the presence of ADP is not consistent with the experimental data, as its inclusion results in a strong negative density peak (colored red).

As this is the first example of nucleotide-free kinesin, we analyzed how this state would be reflected in the structure of the nucleotide pocket. In general, the structure in the vicinity of the nucleotide-binding pocket more closely resembles ADP-bound kinesins, with the switch II helix in the 'down' position (Figure 4A). All conserved amino-acid residues that normally contact bound ADP (P loop and switch II loop) have similar side-chain positions in both ADP-free pKinI and ADP-bound kinesins. The only difference is that, in pKinI, switch II loop residue D236 does not form a highly conserved hydrogen bond with P-loop T99 (see Figure 4C for location of these residues). The absence of this hydrogen bond is explained by the switch II loop backbone being displaced about 1 Å away from the nucleotide-binding pocket towards the MT-binding surface, compared to the ADP-bound kinesin structures. Switch I shows a similar 1 Å shift (Figure 4B), and these two shifts combined could indicate a slight opening of the binding pocket in the absence of nucleotide.

The structures of the switches, and the networks of switch I–II hydrogen bonds, vary greatly among ADP-bound kinesin structures (Kull and Endow, 2002), so it is difficult to draw conclusions from any differences in these regions between pKinI and other kinesin structures. The most notable difference in this region is the two-turn helix in switch II L11, which is stabilized by two hydrogen bonds (Figure 4C): a unique bond between kinesin-required switch I residue R211 and KinI-conserved switch II loop residue D245, and a rare bond between switch I residue S210 and switch II loop residue R242. R242 is usually displaced away from the binding pocket, but it points toward switch I in Kif1a-ADP, so this feature is not unique to pKinI. As a result of these two hydrogen bonds, the pKinI structure lacks the switch I

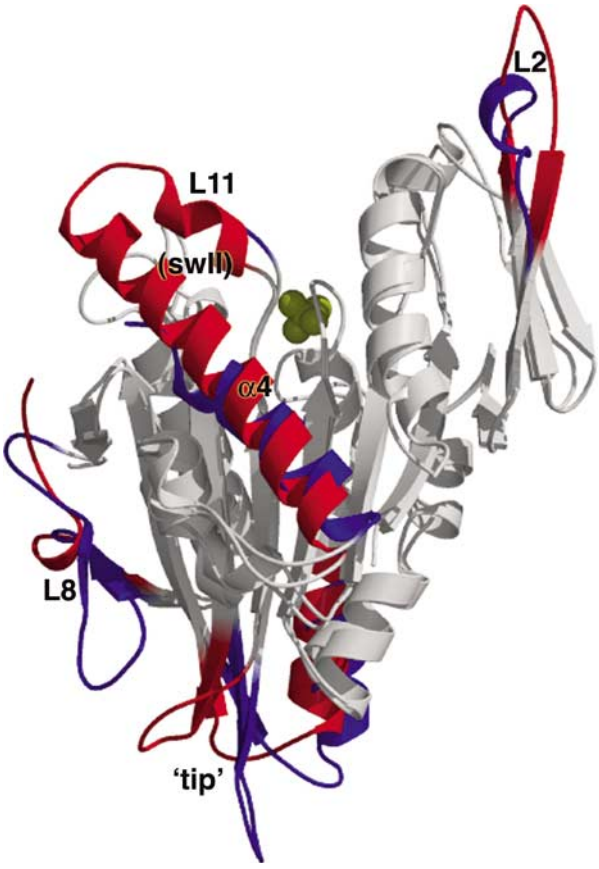

Figure 2 Comparison of pKinI with the most structurally similar gliding motor NCD. Common elements are shown in gray, differing pKinI parts in red and differing NCD parts in blue. The sulfate ion that marks the β-phosphate of ADP is shown in yellow. The largest differences are the length of L2, the positioning of the 'tip' (L6 and L10), the direction of L8 and the unusual stability of the switch II region (L11-α4).

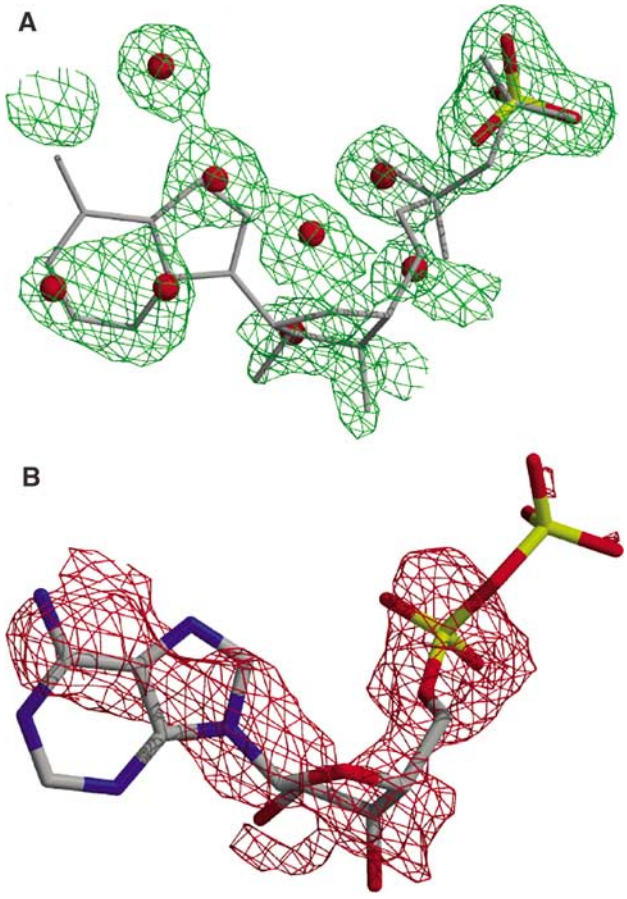

Figure 3 Electron density in pKinI nucleotide-binding pocket shows solvent. (**A**) Green 3Fo-2Fc map (level = 1σ) shows where both the data and model predict density (sulfate and waters—ADP in gray for reference, from Kif1a-ADP model). (**B**) With inclusion of ADP in the pKinI model, and one round of refinement, the red Fo-Fc map (level = −2.5σ) indicates where the model predicts density that the data do not support.

R211–switch II E241 hydrogen bond that had been seen in some kinesin structures.

Besides the slight shift in the switch I and switch II loop backbone, which may indicate a slight opening of the pocket, and the unique R211–D245 hydrogen bond that helps to stabilize switch II, no significant binding-pocket difference is seen between the nucleotide-free pKinI structure and ADP-bound kinesin structures. These observed differences are small compared to the conformational changes found between Kif1a-ADP and Kif1a-AMP-PNP (Kikkawa *et al*, 2001).

Mutational studies on pKinI

As the KinI family performs such a distinct function, we were interested in identifying the residues specifically conserved within the KinI family. Multiple sequence alignment (Supplementary Figure) showed that such residues are located in MT-binding regions of the protein. Three individual KinI-specific residues and two sets of residues were mutated to alanines and assayed for their effects on MT depolymerization and ATP hydrolysis (Figure 5).

Two of the chosen conserved residues, Arg 242 and Asp 245, are located in the switch II loop L11. In the pKinI structure, these residues stabilize L11, which is disordered in most kinesin crystal structures, to form a short helix that precedes the switch II helix α4 (Figure 4C). Interestingly, the stabilizing hydrogen bonds that these residues form are with switch I residues (Ser 210 and Arg 211) that are conserved in all kinesins and crucial to their function (Supplementary Figure).

The other KinI-specific conserved residues that were mutated, KVD (Lys40-Val41-Asp42), KEC (Lys268-Glu269-Cys270) and Arg272, were expected to affect MT or tubulin binding by pKinI. KEC and Arg272 are located in the region proven to be the major MT-binding site for kinesin motors, at the C-terminus of the long switch II helix adjacent to the L12/α5 region (Woehlke *et al*, 1997). KVD is a set of pKinI-conserved amino acids in the family-specific insertion in loop L2, which might also contact the MT based on EM experiments in pKinI (Moores *et al*, 2003) and proteolysis experiments in NCD (Alonso *et al*, 1998).

To analyze how the chosen family-specific residues may confer MT depolymerization activity on a kinesin motor, we assessed the ability of the purified mutant proteins to depolymerize MT. The results of these studies (Figure 6, blue bars) showed that most of the selected residues affect the depolymerization activity of the protein, with KEC and KVD mutants showing no significant depolymerization, and R272A and

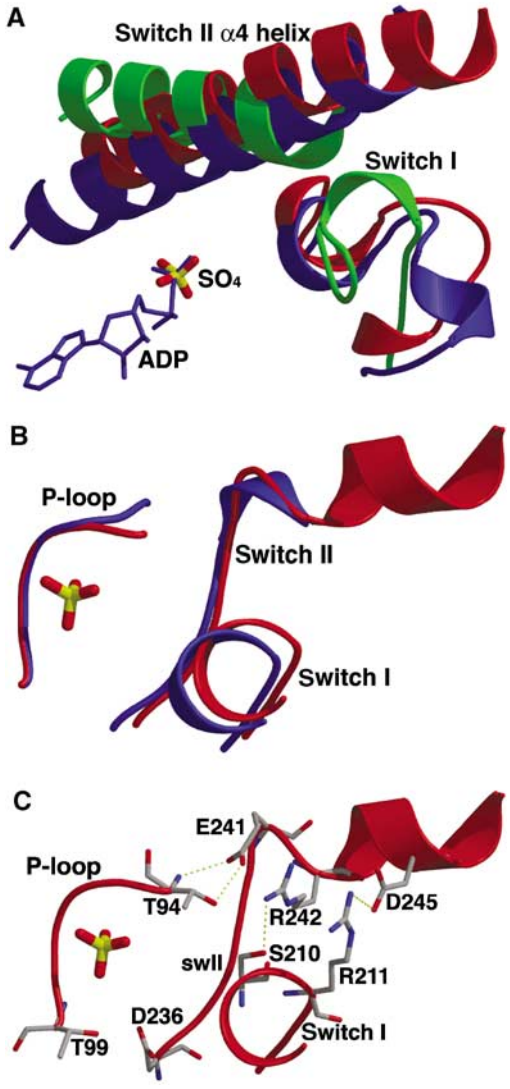

Figure 4 Switches I and II and the binding-pocket region of nucleotide-free pKinI. (**A**) Comparison of switch regions between pKinI (red), Kif1a + ADP (blue) and Kif1a + AMP-PNP (green). Stick models are shown for ADP (blue) and the sulfate from the pKinI model that sits at the β-phosphate position. (**B**) Shift of the switch I and switch II loops of pKinI (red), compared to Kif1a-ADP (blue). This may represent an opening of the binding pocket in the absence of nucleotide, but it is very small. (**C**) pKinI binding-pocket hydrogen bonds, as discussed in the text, between KinI-conserved switch II residues R242/D245 and absolutely conserved switch I residues S210/R211.

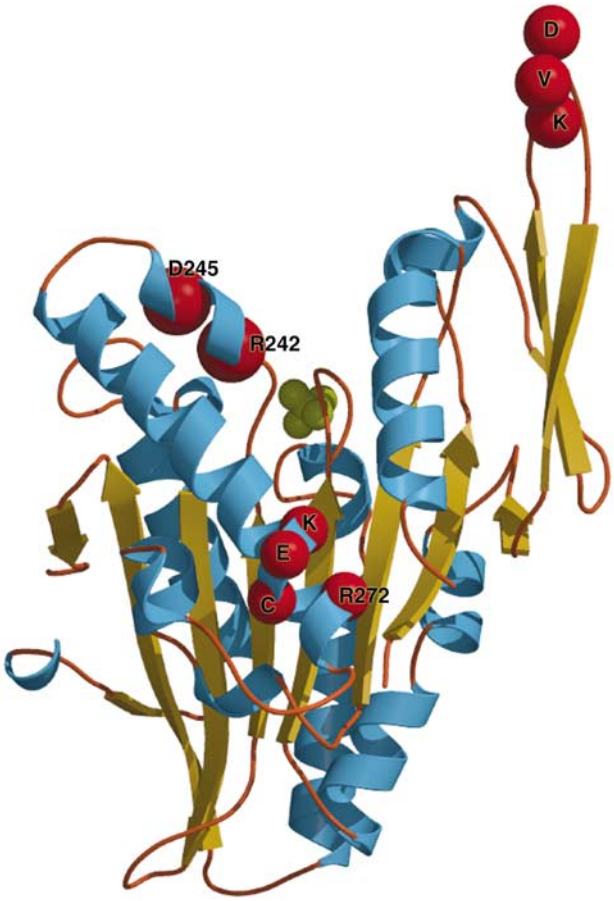

Figure 5 Location of pKinI amino-acid substitutions. Red spheres mark the three residues and two-residue triplets (K40/V41/D42 and K268/E269/C270) that were mutated to alanine and assayed for their effects on ATP hydrolysis and MT depolymerization.

R242A mutants displaying activities significantly lower than that found for wild-type pKinI. One notable exception is the D245A mutant, which depolymerized MT as well as wild-type pKinI.

To further study the interaction of the mutants with MTs, we employed EM methods (Figure 7). In the presence of the nonhydrolyzable ATP analogue AMPPNP, wild-type pKinI forms characteristic motor-tubulin ring structures (circles in Figure 7), which reveal the tubulin deformation mechanism of KinI-catalyzed MT depolymerization (Moores *et al*, 2002). Only one of the pKinI mutants, D245A, formed these ring structures, consistent with its ability to depolymerize MTs with an activity similar to that of wild-type pKinI (Figure 6). We examined the MT-binding activities of the pKinI mutants, both by visual inspection (arrows in Figure 7) and optical diffraction (not shown). The pKinI mutants displayed a range of MT decoration by these criteria—from KEC, which showed essentially no decoration, to KVD, which showed very clear decoration (Figure 7). These results reflect a general trend in the degree to which the alanine substitutions affect the motor's ability to interact with its MT substrate. The KVD mutant was particularly striking in this respect, as it was able to bind the MT lattice (Figure 7) but showed no depolymerization activity (Figure 6).

To determine which steps in the pKinI catalytic cycle are affected by the introduced mutations, we also analyzed the ATPase activities of the mutants (Figure 6), in the presence of either MTs (red bars) or free tubulin dimers (yellow bars). Our results showed that MT and tubulin subunits at concentrations of 100 μg/ml (0.91 μM) equally stimulated ATP hydrolysis by wild-type pKinI. Similar results were obtained in other studies (Hunter *et al*, 2003; Moores *et al*, 2003), confirming that KinI ATPase activity can be stimulated by GDP-bound tubulin dimer. This finding contrasts with the ATPase activities of other kinesin motors, which are highly stimulated by MT but not by tubulin.

In our study, R242A mutant showed only half the ATPase activity of wild-type pKinI, with addition of either MT or tubulin. D245A mutant had ATPase activity similar to wild-type for both MT and tubulin. KEC mutant had almost no

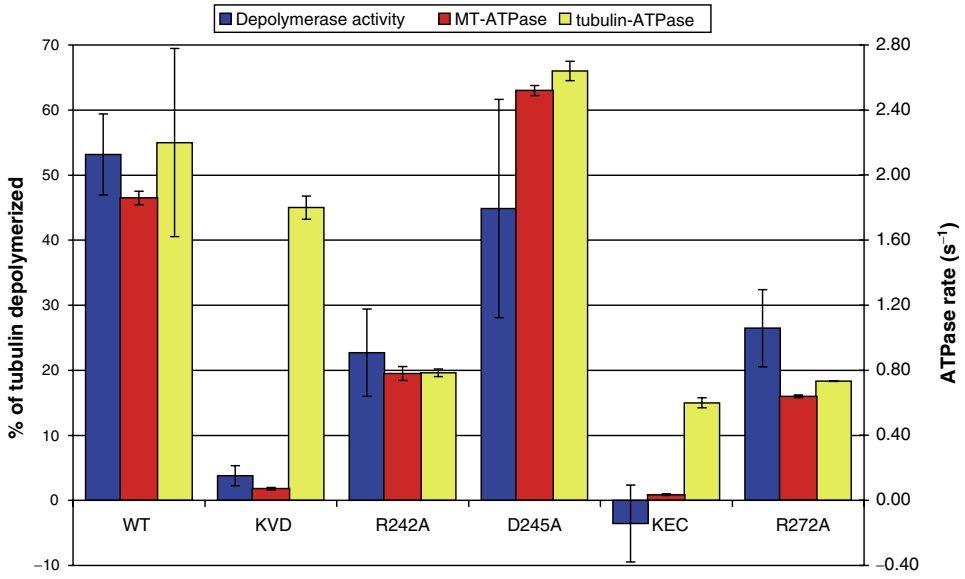

Figure 6 ATPase and depolymerase activities of wild-type pKinI and the alanine mutants. Depolymerization activity is shown by the blue bars. ATPase activity in the presence of MT is shown in red, while ATPase activity in the presence of free tubulin dimer is shown in yellow. Error bars represent one standard deviation. Note the large difference between MT-ATPase and tubulin-ATPase activities seen for KVD, and to a lesser degree for KEC. Note also that decreases in depolymerization activity roughly correlate with decreases in MT-ATPase activity.

activity in the presence of MT, but ~27% activity in the presence of tubulin compared to wild-type pKinI. R272A mutant had only about a third of wild-type activity in the presence of both MT and tubulin. Finally, KVD had very little activity with MT, but retained most of its activity with tubulin. The latter mutant contrasts with the other tested mutants, which showed similar decreases in activity under both conditions.

The pKinI–MT complex

We put these observations concerning the structure and activity of pKinI into the context of its MT interaction by docking our crystal structure into the electron density of a pKinI–ADP–MT map determined using cryo-electron microscopy and helical image analysis (Figure 8; Moores *et al*, 2003). This modeling experiment showed the location of mechanistically significant parts of the motor with respect to the MT surface. We also docked the tubulin heterodimer structure (Löwe *et al*, 2001) into the MT portion of the map to create a pseudo-atomic model of the motor–MT interaction. As with other kinesins, and described previously (Moores *et al*, 2003), pKinI makes its main contacts with the MT surface by interacting with the C-terminal helices H11 and H12 of α- and β-tubulin (in yellow).

The switch II cluster of pKinI (shown in red), which includes the mutated residues R242, D245 in loop l1, and R272 and KEC in α4, abuts the intradimer interface of the αβ-tubulin heterodimer and thus plays a key role in the pKinI–MT interaction. In particular, this explains the reduced binding and ATPase activity of the R242A, R272A and KEC mutants. The absence of effect of the D245A mutation in this key area suggests that this conserved residue is likely to have a role in the context of full-length pKinI. KinI-specific residues may also help to couple ATP binding with movement of the α4 helix between the tubulin subunits of the dimer, bringing about the characteristic KinI ATP-induced deformation of the dimer and subsequent MT depolymerization.

Loop L2, the location of the KVD mutation, is depicted in cyan and lies close to the MT surface. It also lies close to the conformational change that pKinI undergoes when it releases ADP on binding to the MT (black density; Moores *et al*, 2003). As this loop contains a number of KinI-specific residues, it is an ideal structural candidate for participating in KinI-specific functions associated with MT-lattice regulation of pKinI activity (Moores *et al*, 2003) and MT-end-stimulated depolymerization. The fit shown has L2 hanging partially outside the pKinI EM density, strongly supporting the idea that L2 undergoes a conformational rearrangement relative to the crystal structure when initially bound to its MT substrate. The behavior of the KVD mutant also points to the role of L2 in the pKinI bending step of depolymerization, so it is likely to undergo further conformational changes as depolymerization proceeds.

Loops L8 and L12 (in orange) are proposed to be the other major points of contact between kinesins and MTs (Woehlke *et al*, 1997; Alonso *et al*, 1998). The MT surface is not accessible to L8, due to both its unusual conformation and the length of α4 in our pKinI structure, which perhaps reflects a preference for binding instead to the curved tubulin dimer. However, L12, along with L2, is sufficient to form anchor points on the MT surface at either end of the motor, between which the ATP-sensitive switch II components can act directly on the motor substrate.

Discussion

Structure: differences from other kinesins

A unique feature of the pKinI structure is the conformation of switch II. The long switch II helix (α4) is stabilized to be three turns longer than in the NCD structure (Figure 2), and the switch II loop (L11) is stabilized by family-specific residues to

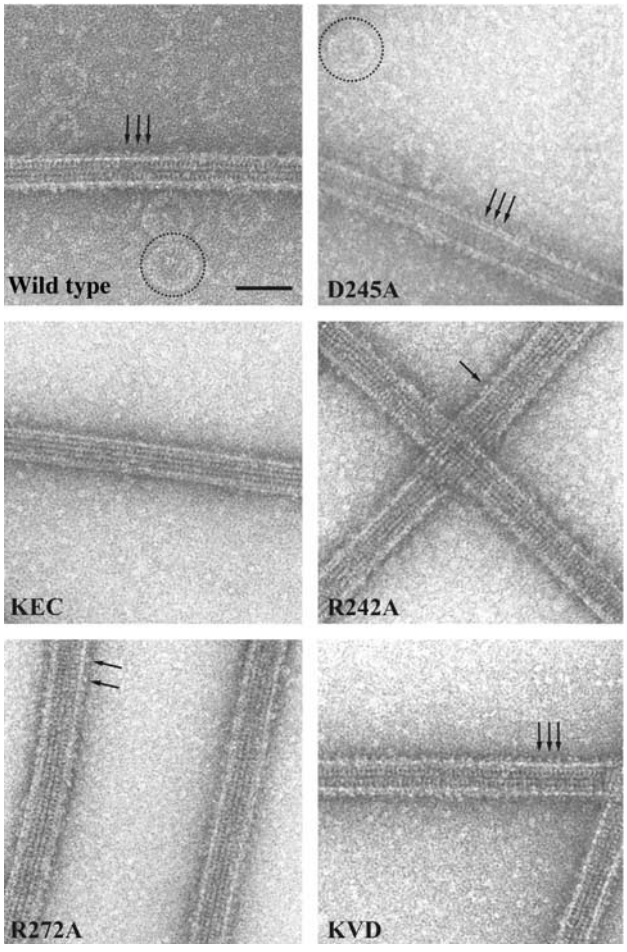

Figure 7 Mutations in the pKinI motor core affect its ability to bind and depolymerize MTs in the presence of the nonhydrolyzable ATP analogue AMPPNP. Each pKinI construct was incubated with AMPPNP and taxol-stabilized MTs; the mixture was centrifuged and the pellet fraction was resuspended and examined by negative stain microscopy. Characteristic motor–tubulin ring complexes, which form under these conditions, are shown by the dotted circles and examples of motors bound along the MT lattice are indicated with arrows. Tubulin oligomers are also observed in the background. Scale bar = 400 Å.

form a short helix (Figure 4C). This stabilization of the switch II region by family-specific residues may be important for pKinI's unique depolymerization activity. However, a long switch II helix and ordered switch II loop have been seen in a few other kinesin structures, such as Kif1a-ADP (Kikkawa *et al*, 2001), so it is difficult to interpret this structural feature in terms of KinI function.

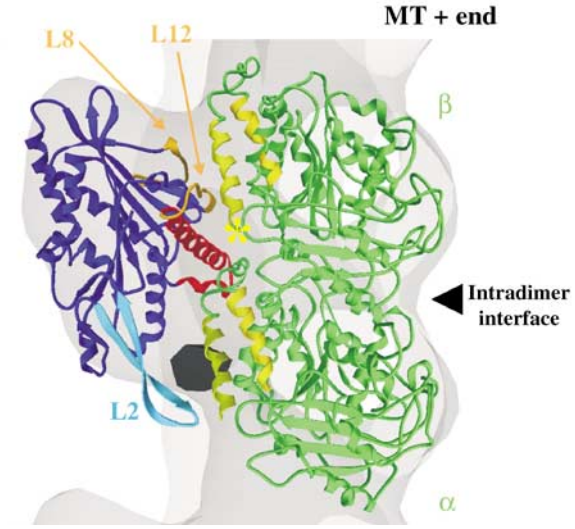

Figure 8 Pseudo-atomic model of the pKinI–MT complex. The crystal structure of pKinI (blue) was docked within the motor density of the pKinI–ADP–MT map (gray). The switch II cluster (including the mutated residues R242, D245 in loop 11 and R272 and KEC on α4) is shown in red, while loop L2 (location of KVD mutation) is depicted in cyan. L2 lies close to the conformational change that pKinI undergoes when it releases ADP on MT binding (black density). Loops 8 and 12 (orange) are proposed to be the other major point of contact between kinesins and MTs. The structure of GTP-tubulin (green) was fit within the MT portion of the map; H11 and H12 helices of α- and β-tubulin are shown in yellow and the position of the disordered β-tubulin C-terminus, essential for pKinI depolymerization, is marked with a yellow asterisk. The figure was prepared by manually docking the coordinates of pKinI and the αβ-tubulin heterodimer (1JFF, Löwe *et al*, 2001) into the pKinI–ADP–MT map using AVS (Advanced Visual Systems).

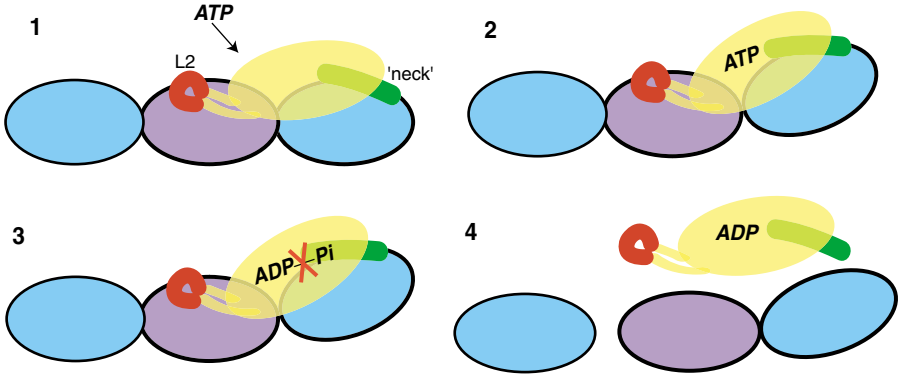

Figure 9 Model of KinI core function. Purple = α-tubulin, light blue = β-tubulin, yellow = KinI catalytic core, red = loop 2, green = region of KinI that attaches to β-tubulin (possibly N-terminal 'neck', L12, L8): (1) When KinI recognizes and binds a tubulin dimer at the end of an MT, L2 binds to α-tubulin, and another KinI element, such as L12 and/or the neck, binds to β-tubulin. The majority of the KinI core binds at the intradimer interface. (2) When ATP binds to KinI, it induces a conformational change in the catalytic core that pulls the tubulins at the L2 and 'neck' attachments and pushes in at the intradimer interface, curving the dimer. (3) With KinI in this new tubulin-binding conformation, ATP hydrolysis is stimulated. (4) ATP hydrolysis weakens the tubulin dimer's connection to the MT, releasing the dimer–KinI complex. It also weakens KinI binding to tubulin, freeing KinI into solution for rebinding and continued depolymerization of MT.

Other specific structural features of pKinI may also relate to its function as a depolymerizing enzyme. The 'arrowhead' tip (L6 and L10) is the site where the neck linker docks on the catalytic core in other kinesins (Sablin *et al*, 1998). The fact that the pKinI tip is bent away from the MT-binding site (Figure 2) suggests that its neck may dock onto the catalytic core in a novel way, possibly accommodating a better fit of the motor to the curved surface of the tubulin protofilament. The opposite pole of the motor is distinguished by the long loop L2 that contains family-specific insertions (Figures 2 and 5), and our docking experiment demonstrates that this region is involved in specific interactions with the MT. The structure of L8, another MT-binding loop, might also be related to pKinI function. The unique configuration of this loop could reduce normal kinesin–MT interactions and allow a better fit to curved tubulin.

Structure: lack of nucleotide

A surprising feature of the pKinI structure is the absence of the nucleotide in the binding pocket. The first structure of myosin S1 also had sulfate in place of nucleotide (Rayment *et al*, 1993), and additional myosin structures have been obtained in this state as well as other nucleotide states (Houdusse *et al*, 2000; Coureux *et al*, 2003), but this is the first such kinesin structure found. Moreover, although many crystallization conditions were tried with numerous ATP/ADP analogues, we have not yet been able to grow pKinI crystals with nucleotide bound.

Kinetic data suggest that ADP release in the absence of MT is much faster for pKinI than for all other kinesins analyzed (M Hekmat-Nejad, manuscript in preparation), which might explain the absence of bound nucleotide in the pKinI pocket. However, although some binding-pocket residues differ between KinI and other kinesins (Supplementary Figure), there is no difference striking enough to explain how the local environment could lead to pKinI's lower affinity for ADP. In addition, it is possible that our crystallization conditions, a combination of high sulfate (1.6 M) and low pH, might have also helped to shift the protein toward the nucleotide-free state, by providing the sulfate ion that occupies the binding pocket. However, a nucleotide-free structure was not obtained for human conventional kinesin at a similar sulfate concentration (Sindelar *et al*, 2002). The nucleotide-free pKinI structure is probably a reflection of both high-sulfate conditions and possible lower affinity for ADP, and we do not expect that this state would predominate under more *in vivo* conditions.

Our analysis of the key elements in the nucleotide-binding pocket (Figure 4) suggests that the pKinI crystal structure has essentially an ADP-like conformation. It is difficult to draw further conclusions from this fact, because the nucleotide state and structural state are often unrelated for crystal structures of both kinesins and myosins; some ADP-bound structures display an ATP-like state, apparently because the barrier between the ADP-like and ATP-like states is low in the absence of their respective polymer substrate (MT or actin) (Kikkawa *et al*, 2001). A structure of KinI in a more radically altered, ATP-like state is desirable in order to understand better the conformational changes that occur during the KinI nucleotide cycle.

pKinI ATPase activity: tubulin versus MT

Plasmodium KinI ATPase activity increases in the presence of tubulin dimer as well as MT. These results are consistent with the recent finding that MCAK ATPase activity is enhanced in the presence of free tubulin dimers (Hunter *et al*, 2003). However, in contrast to the results with full-length MCAK, which showed relatively low ATPase activity in the presence of tubulin compared to MTs, the ATPase activity of pKinI catalytic core was comparable in the presence of 100 μg/ml (0.91 μM) of MT and tubulin. The most likely explanation for this difference in relative activities is that the non-core portions of full-length KinI, which are not present in our construct, might help the motor to distinguish polymer ends from free tubulin dimers, increasing the enzyme's efficiency. Supporting this, pKinI ATPase activity is actually inhibited at higher concentrations of MT (Moores *et al*, 2003); similar results are seen for the mutants with significant MT-stimulated ATPase (R272A, R242A, D245A—data not shown).

pKinI mutants: strategy

pKinI has a number of characteristic properties, which include MT depolymerization, ATPase stimulation by both polymerized and unpolymerized tubulin, binding to the MT lattice and the ability to form tubulin–motor ring complexes in the presence of the nonhydrolyzable ATP analogue AMPPNP. All these properties likely reflect the aspects of a general KinI depolymerizing mechanism. The crystal structure of pKinI provided us with the opportunity to visualize the location of KinI-specific residues. We mutated a number of these residues and tested for the above activities, and were able to develop a consistent view of the role that these residues might play in the KinI mechanism.

pKinI mutants: MT-depolymerizing loop 2 (KVD)

In the KinI family, L2 has an insert of highly conserved family-specific residues (K40-V41-D42) (Supplementary Figure), so this region was expected to be especially important for the family's unique function. The KVD mutant, with the three L2 residues mutated to alanine, showed only a small reduction in ATPase activity in the presence of free tubulin dimer (Figure 6), indicating that the protein's ATP binding and hydrolysis apparatus was relatively unaffected, along with its ability to bind tubulin in order to stimulate hydrolysis. EM results also showed that this mutant could bind MT well. However, it showed very little if any depolymerization activity, paralleling its low ATPase activity in the presence of MTs. As the very low depolymerization rate for KVD is not due to changes in the ATP hydrolysis machinery itself, or an inability to bind MTs or tubulin, this family-specific insertion in L2 is the first region identified as specific for initiating MT depolymerization.

A pseudo-atomic model of the pKinI–MT complex (Figure 8) demonstrated that L2 is located close to the MT surface, as has been shown for this region in other kinesin family members (Sosa *et al*, 1997; Kikkawa *et al*, 2001). However, the mobility of this region suggested by the docking, and the proximity of L2 to a site of significant conformational change during the motor's ATPase cycle, support a specific role for L2 in pKinI regulation and depolymerization.

pKinI mutants: MT-binding switch II helix (KEC and R272)

Four KinI-conserved residues were mutated in the central kinesin–MT binding site (α4). Mutating KEC to alanine led to essentially no depolymerization or ATP hydrolysis in the

presence of MT, and a substantial decrease in ATPase activity in the presence of free tubulin (Figure 6). EM images show that KEC barely decorates the MT (Figure 7). The latter results strongly suggest that the low depolymerization activity seen for this mutant is due to its lowered ability to bind MT. The alanine mutant of R272, the residue that emanates from α4 one helical turn below KEC (Figure 5), shows similar assay results (Figure 6), supporting a similar role of this residue in MT binding, while our docking experiment clearly demonstrates the proximity of these residues to the MT surface. The lesser effect of the R272A mutation on MT binding and ATP hydrolysis is likely due to only one residue being mutated, instead of three in the KEC mutant. Similar ATPase activities of these mutants in the presence of free tubulin, as compared to R242A, suggest that both mutants partially retain their ability to bind tubulin in its curved form.

pKinI mutants: nucleotide-contacting switch II loop (R242 and D245)

In pKinI, the switch II loop, which links the bound nucleotide to the conformation of the MT-binding site (Song and Endow, 1998), contains two family-conserved residues, R242 and D245. R242A mutant showed about half the wild-type activity for depolymerization and for ATP hydrolysis in the presence of both MT and tubulin (Figure 6), and EM results also showed that the ability of this mutant to depolymerize is partially impaired (Figure 7). However, although R242 is absolutely conserved in the KinI family, the basic amino acids at this position are not unique to KinI (Supplementary Figure). This suggests that, unlike KVD, R242 is not specifically important for depolymerization. This idea is supported by the general reduction in ATP hydrolysis activity for R242A, which points toward the mutant having its primary effect on hydrolysis, and affecting depolymerization only as a result of this. R242A mutant can still bind to MT (Figure 7), and the residue is close to the binding pocket and hydrogen bonds with an important switch I residue (Figure 4C), suggesting that R242 plays a more direct role in ATP hydrolysis, and possibly MT binding as well, but to a smaller degree (Figure 8).

For the D245A mutant, depolymerization and ATPase activities, in the presence of either MT or tubulin, are not reduced by the alanine substitution. It is possible that D245, which is conserved only in the KinI family, plays its role in the activity of full-length dimeric KinI. Most other kinesins have a basic residue at this site, suggesting that negatively charged D245 might help to reduce nonproductive binding of KinI to the MT surface. In addition to this residue, the other parts of the full-length KinI protein, especially the ~60 aa neck domain, might be important for targeting the motor to the ends of the MT, so that nonproductive binding does not occur and depolymerization efficiency is maximized.

pKinI ATP hydrolysis requires binding to curved tubulin dimer

Studying ATPase activity in the presence of either MT or tubulin dimers allowed us to further compare the pKinI mutants. They are of into two types: those that decrease KinI ATPase activity to the same degree under both conditions (R242A, R272A), and those that decrease the activity more in the presence of MT (KEC, KVD) (Figure 6). KVD is especially striking for the discrepancy in its relative activity between the two conditions. The combined results of these studies show a general pattern: the relative depolymerization activity of each test mutant is very similar to its relative MT-stimulated ATPase activity. In particular, KVD mutant has intact ATP hydrolysis machinery, as seen in the tubulin assay, but can neither depolymerize MTs nor hydrolyze ATP when bound to them (Figure 6).

Earlier studies showed that KinI bound to nonhydrolyzable AMP-PNP induces curvature in stabilized MTs (Desai *et al*, 1999; Moores *et al*, 2002), supporting the idea that MT curvature occurs before ATP hydrolysis and not at the same time. This, along with our results, suggests that the motor domain only hydrolyzes ATP when bound to curved tubulin, either as free GDP-bound dimers, or at the ends of MTs where curvature has been induced to start depolymerization. This suggests a model for the enzyme's mechanism: KinI binds to the straight tubulin protofilament, but cannot hydrolyze ATP until it has forced the tubulin dimer to which it is attached to become curved, that is, until it has initiated depolymerization. Only then can it hydrolyze ATP and release itself from the tubulin surface. Thus, the only difference between ATPase activity in the presence of MT and of free tubulin dimer is that the MT must be depolymerized first.

Model for KinI core-domain function

Based on the combined results of our structural and mutational studies, we present here revisions to the KinI mechanism (Figure 9). We propose that when KinI has reached the MT end and lost its ADP nucleotide, the switch II cluster makes the major contact with tubulin at the interdimer interface, while the family-specific L2 residues and the N-terminal 'neck' domain (along with L12 and possibly L8), which are located at opposite ends of the catalytic core (Figure 9), provide anchor points around the switch II cluster.

ATP binding induces a conformational change that results in L2, the neck and L12 (and maybe also L8) tugging and bending the tubulin protofilament underneath. In the resulting 'curved' tubulin conformation, contacts between the KinI and the tubulin dimer are maximized, perhaps by enabling L8 to contact tubulin. This stabilizes the activation state, triggering hydrolysis of the ATP. After ATP hydrolysis, the KinI binding to the tubulin dimer is weakened, leaving KinI free in solution to bind another MT protofilament and further catalyze depolymerization.

Materials and methods

Crystallization and model determination

Cloning, expression and purification of the motor domain of MCAK from *P. falciparum* are described in Moores *et al* (2002) (Supplementary data). Protein fractions of >95% purity were pooled and concentrated to 10–20 mg/ml. Crystals were grown in sitting drops by mixing equal volume of protein solution with well solution containing 1.4–1.8 M ammonium sulfate, 100 mM sodium acetate (pH 5.0) and 200 mM sodium nitrate. Crystals typically appeared in 1–2 days and were harvested after growth of 1–2 weeks at 4°C. Crystals (typically $100 \times 50 \times 50\,\mu m^3$) were transferred to well solution containing 30% glycerol and then frozen in liquid nitrogen. Diffraction data were collected at beamline 9-1 at SSRL and 8.3.1 at ALS. At least 10 different data sets were collected in an effort to obtain crystals with nucleotide bound to the protein. All attempts were unsuccessful, as judged by the electron density maps obtained by molecular replacement methods. The structure presented here reflects data collected at ALS beamline 8.3.1. The data were processed with DENZO and SCALEPACK (Otwinowski

and Minor, 1997) and the structure was solved by molecular replacement methods using CNS programs (Brunger *et al*, 1998) and the KAR3 structure (Yun *et al*, 2001; PDB code 1F9T) as a search model. The model was built using QUANTA (Accelrys) and refined using CNS programs, with three final rounds of refinement using Refmac 5.1.24 (Collaborative Computational Project No. 4, 1994) and validation using PROCHECK (Laskowski *et al*, 1993). Figures were prepared using Bobscript v2.4 (Esnouf, 1997). The model presented here contains 318 amino acids, 306 waters and one sulfate. It has working $R = 0.202$ and $R_{free} = 0.230$. Residues 157–167 are disordered. It has been submitted to the PDB and is accessible with reference code 1RY6.

Preparation of pKinI mutants

Point mutations were introduced using the QuikChange kit (Stratagene). Proteins were purified as described by Moores *et al* (2002) (Supplementary data).

ATPase assay

The ATPase activity of pKinI was measured using the NADH-coupled system of Huang and Hackney (1994). Initial rates of MT- or tubulin-stimulated ATP hydrolysis by pKinI were measured at several different pKinI concentrations ranging from 5 to 40 μg/ml (0.12–0.98 μM) at room temperature in BrB25 buffer consisting of 25 mM Pipes (pH 6.8), 2 mM $MgCl_2$, 1 mM EGTA, 1 mM DTT, and with 1.5 mM ATP, 100 μg/ml MTs or 100 μg/ml tubulin subunits (0.91 μM for tubulin dimer subunits, both free and in polymer). Results are shown for 10 μg/ml (0.25 μM) pKinI.

Microtubule depolymerization assay

All concentrations are final in the reaction mixture. MTs were polymerized from purified, prespun porcine tubulin at 37°C for 30 min in the presence of 1.2 mM GTP, 1 mM DTT and 10% DMSO, followed by another 5-min incubation at 37°C with 20 μM taxol. Polymerized MTs were spun over 1 ml of sucrose cushion consisting of 40% sucrose in BrB25 buffer with 20 μM taxol in 1-ml aliquots at 25°C. MT pellets were washed and resuspended in BrB25 buffer with 20 μM taxol. In all, 20 μg/ml *Plasmodium* KinI (0.49 μM) was incubated with 200 μg/ml (1.8 μM) of purified MTs in the presence of 3 mM ATP or 5 mM ADP and 10 units/ml of apyrase (in this case, pKinI was preincubated with ADP and apyrase for 15 min prior to the addition of the MTs), or with no nucleotide added for 15 min at room temperature. MT polymers were separated from tubulin subunits by ultracentrifugation of 150 μl of the reaction mixture at 55 000 RPM in a TLA-100 rotor at 25°C for 15 min. Aliquots of the samples prior to ultracentrifugation, the supernatant and pellet fractions were analyzed by SDS–PAGE. Tubulin bands on coomassie-stained gels were quantified using the Fluorchem digital imaging system (Alpha Innotech Corporation).

The molecular weights used for calculating the molar concentrations of pKinI and tubulin dimers are 40 711 and 110 000, respectively. '% tubulin depolymerized' shown in Figure 6 was calculated by determining the percentage of free tubulin (tubulin in S/(tubulin in S + tubulin in P)) for the reactions incubated with pKinI and ATP, and subtracting from this the percentage of free tubulin from the reactions with no pKinI. This yielded the percentage of tubulin that was depolymerized actively, rather than through MT dynamic instability.

Electron microscopy of pKinI mutants and MTs

pKinI mutants incubated with AMPPNP (ICN) and taxol-stabilized MTs were prepared as described in Moores *et al* (2002). The concentration of polymerized tubulin in the assay was 5 μM and of each of the constructs was: wild-type pKinI 11 μM, D245A 17 μM, R242A 24 μM, KEC 6 μM, R272A 10 μM and KVD 7 μM.

Supplementary data

Supplementary data are available at *The EMBO Journal* Online.

Note added in proof

A recent paper by Ogawa *et al* in *Cell* provides structures of a KinI that include the N-terminal neck. The neck is positioned differently from other kinesin models, suggesting that it is important for targeting to the MT end. This paper also affirms the importance of L2 and the idea that KinI hydrolyzes ATP on curved tubulin dimer (Ogawa *et al*, 2004).

Acknowledgements

We thank Elena Sablin for many helpful comments on this manuscript. C Moores thanks B Sheehan (The Scripps Research Institute) for help with preparing Figure 8. This work was supported by grants from the National Institutes of Health (PO1-AR42895, GM52468). K Shipley is supported by a Howard Hughes Predoctoral Fellowship.

References

Aizawa H, Sekine Y, Yakemura R, Zhang Z, Nangaku M, Hirokawa N (1992) Kinesin family in murine central nervous system. *J Cell Biol* **119:** 1287–1296

Alonso MC, van Damme J, Vandekerckhove J, Cross RA (1998) Proteolytic mapping of kinesin/ncd-microtubule interface: nucleotide-dependent conformational changes in the loops L8 and L12. *EMBO J* **17:** 945–951

Brunger AT, Adams PD, Clore GM, DeLano WL, Gros P, Grosse-Kunstleve RW, Jiang J-S, Kuszewski J, Milges M, Pannu NS, Read RJ, Rice LM, Simonson T, Warren GL (1998) *Crystallography & NMR System*: a new software suite for macromolecular structure determination. *Acta Crystallogr D* **54:** 905–921

Collaborative Computational Project No. 4 (1994) The CCP4 suite: programs for protein crystallography. *Acta Crystallogr D* **50:** 760–763

Coureux P-D, Wells AL, Menetrey J, Yengo CM, Morris CA, Sweeney HL, Houdusse A (2003) A structural state of the myosin V motor without bound nucleotide. *Nature* **425:** 419–423

Desai AS, Mitchison TJ (1997) Microtubule polymerization dynamics. *Annu Rev Cell Dev Biol* **13:** 83–117

Desai AS, Verma S, Mitchison TJ, Walczak CE (1999) Kin I kinesins are microtubule-destabilizing enzymes. *Cell* **96:** 69–78

Esnouf RM (1997) An extensively modified version of MolScript that includes greatly enhanced coloring capabilities. *J Mol Graphics* **15:** 132–134

Homma N, Takei Y, Tanaka Y, Nakata T, Terada S, Kikkawa M, Noda Y, Hirokawa N (2003) Kinesin superfamily protein 2A (KIF2A) functions in suppression of collateral branch extension. *Cell* **114:** 229–239

Houdusse A, Szent-Györgyi AG, Cohen C (2000) Three conformational states of scallop myosin S1. *Proc Natl Acad Sci USA* **97:** 11238–11243

Huang TG, Hackney DD (1994) *Drosophila* kinesin minimal motor domain expressed in *Escherichia coli*. *J Biol Chem* **269:** 16493–16501

Hunter AW, Caplow M, Coy DL, Hancock WO, Diez S, Wordeman L, Howard J (2003) The kinesin-related protein MCAK is a microtubule depolymerase that forms an ATP-hydrolyzing complex at microtubule ends. *Mol Cell* **11:** 445–457

Inoué S, Salmon ED (1995) Force generation by microtubule assembly/disassembly in mitosis and related movements. *Mol Biol Cell* **6:** 1619–1640

Kikkawa M, Sablin EP, Okada Y, Yajima H, Fletterick RJ, Hirokawa N (2001) Switch-based mechanism of kinesin motors. *Nature* **411:** 439–445

Kline-Smith SL, Walczak CE (2002) The microtubule-destabilizing kinesin XKCM1 regulates microtubule dynamic instability in cells. *Mol Biol Cell* **13:** 2718–2731

Kull FJ, Endow SA (2002) Kinesin: switch I & II and the motor mechanism. *J Cell Sci* **115:** 15–23

Laskowski RA, MacArthur MW, Moss DS, Thornton JM (1993) PROCHECK: a program to check the stereochemistry of protein structures. *J Appl Crystallogr* **26:** 283–291

Löwe J, Li H, Downing KH, Nogales E (2001) Refined structure of αβ-tubulin at 3.5 Å resolution. *J Mol Biol* **313:** 1045–1057

Mandelkow E, Hoenger A (1999) Structures of kinesin and kinesin–microtubule interactions. *Curr Opin Cell Biol* **11:** 34–44

Maney T, Wagenbach M, Wordeman L (2001) Molecular dissection of the microtubule depolymerizing ability of mitotic centromere-associated kinesin. *J Biol Chem* **276:** 34753–34758

McDonald HB, Stewart RJ, Goldstein LS (1990) The kinesin-like ncd protein of *Drosophila* is a minus end-directed microtubule motor. *Cell* **63:** 1159–1165

Moores C, Hekmat-Nejad M, Sakowicz R, Milligan RA (2003) Regulation of KinI kinesin ATPase activity by binding to the microtubule lattice. *J Cell Biol* **163:** 963–971

Moores CA, Yu M, Guo J, Beraud C, Sakowicz R, Milligan RA (2002) A mechanism for microtubule depolymerization by KinI kinesins. *Mol Cell* **9:** 903–909

Muller J, Marx A, Sack S, Song YH, Mandelkow E (1999) The structure of the nucleotide-binding site of kinesin. *Biol Chem* **380:** 981–992

Niederstrasser H, Salehi-Had H, Gan EC, Walczak C, Nogales E (2002) XKCM1 acts on a single protofilament and requires the C terminus of tubulin. *J Mol Biol* **316:** 817–828

Ogawa T, Nitta R, Okada Y, Hirokawa N (2004) A common mechanism for microtubule destabilizers—M type kinesins stabilize curling of the protofilament using the class-specific neck and loops. *Cell* **116:** 591–602

Okada Y, Hirokawa N (2000) Mechanism of the single-headed processivity: diffusional anchoring between the K-loop of kinesin and the C terminus of tubulin. *Proc Natl Acad Sci USA* **97:** 640–645

Otwinowski Z, Minor W (1997) Processing of X-ray diffraction data collected in oscillation mode. *Methods Enzymol* **276:** 307–326

Ovechkina Y, Wagenbach M, Wordeman L (2002) K-loop insertion restores microtubule depolymerizing activity of a 'neckless' MCAK mutant. *J Cell Biol* **159:** 557–562

Rayment I, Rypniewski WR, Schmidt-Bäse K, Smith R, Tomchick DR, Benning MM, Winklemann DA, Wesenberg G, Holden HM (1993) Three-dimensional structure of myosin subfragment-1: a molecular motor. *Science* **261:** 50–58

Rice S, Lin AW, Safer D, Hart CL, Naber N, Carragher BO, Cain SM, Pechatnikova E, Wilson-Kubalek EM, Whittaker M, Pate E, Cooke R, Taylor EW, Milligan RA, Vale RD (1999) A structural change in the kinesin motor protein that drives motility. *Nature* **402:** 778–784

Rogers GC, Rogers SL, Schwimmer TA, Ems-McClung SC, Walczak CE, Vale RD, Scholey JM, Sharp DJ (2004) Two mitotic kinesins cooperate to drive sister chromatid separation during anaphase. *Nature* **427:** 364–370

Sablin EP, Case RB, Dai SC, Hart CL, Ruby A, Vale RD, Fletterick RJ (1998) Direction determination in the minus-end-directed kinesin motor ncd. *Nature* **395:** 813–816

Segerman B, Larsson N, Holmfeldt P, Gullberg M (2000) Mutational analysis of Op18/stathmin–tubulin-interacting surfaces. *J Biol Chem* **275:** 35759–35766

Sindelar CV, Budny MJ, Rice S, Naber N, Fletterick R, Cooke R (2002) Two conformations in the human kinesin power stroke defined by X-ray crystallography and EPR spectroscopy. *Nat Struct Biol* **9:** 844–848

Song H, Endow SA (1998) Decoupling of nucleotide- and microtubule-binding sites in a kinesin mutant. *Nature* **396:** 587–590

Sosa H, Dias DP, Hoenger A, Whittaker M, Wilson-Kubalek E, Sablin E, Fletterick RJ, Vale RD, Milligan RA (1997) A model for the microtubule–Ncd motor protein complex obtained by cryo-electron microscopy and image analysis. *Cell* **90:** 217–224

Thorn KS, Ubersax JA, Vale RD (2000) Engineering the processive run length of the kinesin motor. *J Cell Biol* **151:** 1093–1100

Turner J, Anderson R, Guo J, Beraud C, Fletterick R, Sakowicz R (2001) Crystal structure of the mitotic spindle kinesin Eg5 reveals a novel conformation of the neck-linker. *J Biol Chem* **276:** 25496–25502

Vale RD, Fletterick RJ (1997) The design plan of kinesin motors. *Annu Rev Cell Dev Biol* **13:** 745–777

Vale RD, Reese RS, Sheetz MP (1985) Identification of a novel force-generating protein, kinesin, involved in microtubule-based motility. *Cell* **42:** 39–50

Walczak CE (2000) Microtubule dynamics and tubulin interacting proteins. *Curr Opin Cell Biol* **12:** 52–56

Wang Z, Sheetz MP (2000) The C-terminus of tubulin increases cytoplasmic dynein and kinesin processivity. *Biophys J* **78:** 1955–1964

Woehlke T, Ruby AK, Hart CL, Ly B, Hom-Booher N, Vale RD (1997) Microtubule interaction site of the kinesin motor. *Cell* **90:** 207–216

Wordeman L, Mitchison TJ (1995) Identification and partial characterization of mitotic centromere-associated kinesin, a kinesin-related protein that associates with centromeres during mitosis. *J Cell Biol* **128:** 95–104

Yun M, Zhang X, Park C-G, Park H-W, Endow SA (2001) A structural pathway for activation of the kinesin motor ATPase. *EMBO J* **20:** 2611–2618

